EXPERIMENTAL INVESTIGATION OF GAP INSTABILITY AND GAP VORTEX STREET DEVELOPMENT IN AN ECCENTRIC ANNULAR CHANNEL

George H. Choueiri & Stavros Tavoularis

Department of Mechanical Engineering, University of Ottawa, Ottawa, Canada

Abstract The onset of gap instability and the development of a gap vortex street in the narrow gap region of an eccentric annular channel have been documented using two-component laser Doppler velocimetry and stereoscopic particle image velocimetry. Reported results include the frequency and amplitude of the cross-gap velocity fluctuations as well as cross-sectional velocity maps, which provide a global view of cross-channel mixing.

Introduction − Compound channels containing subchannels connected through narrow gaps include nuclear reactor rod-bundles, double-pipe heat exchangers, inundated rivers, catheterized arteries and other technological and natural systems. Under certain conditions, flows in such channels are prone to a particular type of instability, recently termed *gap instability* [1], which leads to the formation of a *gap vortex street* [1], with pairs of staggered vortices of alternating direction forming on either side of the narrow gap, in a manner that is analogous in some ways to the von Kármán vortex street. The result of cross-gap flows induced by these vortices is a greatly enhanced inter-subchannel mixing, and an increase in cross-gap heat and mass transfer. In the case of a tightly-packed rod bundle, which contains multiple subchannels, the individual vortex streets across each narrow gap are coupled and form a *rod bundle vortex network* [1]. A thorough historical overview of early misconceptions and the recognition of the nature of this phenomenon has been presented by Meyer [2]. Most of the published literature on this topic is concerned with relatively large Reynolds number flows, in which the flow is fully turbulent, *e.g.*, [3,4]. Two experimental studies have been conducted in laminar and possibly transitional flows in annular-like channels [4,5], but both were based on flow visualization and did not report details of the velocity field or the development of gap instability and vortex street. The objective of the present research is to document the patterns of flows in eccentric annular channels and rod bundles under laminar, transitional and turbulent flow conditions; the effects of channel geometry and inlet conditions are also investigated. In the following, we will present results for flow though an annular channel with a diameter ratio $D_o / D_i = 0.5$ and eccentricity $e = 2\Delta y/(D_o - D_i) = 0.8$, where $D_o = 50.8$ mm and $D_i = 24.5$ mm are, respectively, the outer and inner diameters and Δy is the distance between the axes of the inner and outer cylinders.

Experimental Facility and Instrumentation − The test section (see Fig 1.) comprises a clear acrylic annular channel, 1.45 m long, having a square outer cross-section, a machined cylindrical cavity 5.08 cm in diameter, and containing an acrylic rod, which could be traversed to the full range of eccentricities. The refractive index of the fluid, a solution of ammonium thiocyanate, matched that of acrylic material; its viscosity was measured independently and corrected for temperature variations. The flow rate was measured with calibrated transit-time ultrasonic flow meters. Time-resolved local flow velocity was measured with a two-component Laser Doppler velocimeter (LDV) and cross-sectional velocity maps were recorded with a stereoscopic particle image velocimeter (SPIV). The LDV and SPIV measurements were taken at different times, with the flow management devices in the upstream tank and the eccentricity adjusted independently. As it was found that the flow in the test section was very sensitive to these settings, bulk velocity values obtained by the LDV and SPIV systems could not be matched precisely, although they were measured fairly accurately.

Results and Discussion − For the reported LDV measurements, the bulk velocity was $U_b = 0.43$ m/s, whereas for the SPIV measurements $U_b = 0.46$ m/s; the corresponding Reynolds numbers were Re = $D_h U_b / \nu = 7800$ and 8700 ($D_h = D_o - D_i$ is the hydraulic diameter and ν is the kinematic viscosity). Figure 2 shows time-averaged axial velocity contours in a cross-section at $x/D_h = 54.2$ downstream from the inlet, where both the main flow and the gap vortex street were fully developed. The time-averaged flow was symmetric about the plane of geometrical symmetry. The maximum time-averaged velocity in the channel occurred in the wide gap and it was $1.24U_b$, whereas the corresponding peak velocity in the narrow gap was only $0.57U_b$. Cross- and axial velocity measurements at the centre of the gap were taken by traversing slowly (*i.e.,* at a speed equal to $0.003U_b$) the LDV probe along the test section. Figure 3 (top) shows the result of the entire traverse. As the flow developed, the centre-gap axial velocity decreased rapidly from a value near U_b at the inlet to about $0.08U_b$ at $x/D_h = 13$; it remained fairly constant for $13 < x/D_h < 22$, and then it increased again. The axial velocity fluctuations remained relatively small (of the order of $0.04U_b$) until the probe reached $x/D_h = 24.5$, where strong positive fluctuations started building up to reach about $0.60U_b$ on average at $x/D_h = 43$, and then they maintained a fairly constant level. The cross-gap flow velocity fluctuated slightly around a near-zero mean until the probe reached $x/D_h = 19$, beyond which the fluctuation amplitude increased monotonically and levelled to $0.33U_b$ at $x/D_h = 38$. Figure 3 (bottom) shows samples of the cross- and axial velocity time histories at $x/D_h = 51.5$, where the fluctuations had reached their quasi-asymptotic levels. Both signals had a quasi-periodic appearance, but the frequency of the axial fluctuations was twice that of that of the cross-flow. The latter observation was confirmed by the corresponding power spectra, shown in Fig. 4. The Strouhal number of the cross-flow fluctuations was St = $fD_i/U_b = 0.066$. Figure 5 shows two representative velocity maps at x/D_h = 54.2. Unlike the time-averaged results (Fig. 2), the instantaneous flow patterns were strongly asymmetric and also reveal the presence of turbulence at a scale that is significantly smaller than D_h. Results not shown here document that the observed flow patterns are associated with a gap vortex street and Fig. 5 shows clear evidence that the gap vortex street not only has a significant local effect in the gap region, but also strongly influences the global flow dynamics. The axial velocity maximum swings widely across the symmetry plane and the entire channel experiences strong, quasi-periodic velocity fluctuations, in addition to conventional turbulence.

Conclusions – Gap instability was seen to get initiated and develop in the narrow gap of an annular channel, following development of large velocity differences between the gap region and the rest of the channel. Sufficiently downstream of the inlet, a quasi-periodic flow pattern was established, with the entire cross-section subjected to oscillatory flows.

References

[1] Tavoularis, S.. Rod bundle vortex networks, gap vortex streets, and gap instability: a nomenclature and some comments on available methodologies, Nucl. Eng. Des., **241**(11), 4612-4614, 2011.

[2] Meyer, L.. From discovery to recognition of periodic large scale vortices in rod bundles as source of natural mixing between subchannels - a review. Nucl. Eng. Des., **240**,1575–1588, 2010.

[3] Guellouz, M.S. and S. Tavoularis. The structure of turbulent flow in a rectangular channel containing a cylindrical rod - Part 1: Reynolds-averaged measurements, and Part 2: Phase-averaged measurements, Exper. Thermal Fluid Sci. **23**, 59-73 and 75-91, 2000.

[4] Gosset, A. and S. Tavoularis. Laminar flow instability in a rectangular channel with a cylindrical core. Phys. Fluids, 18044108, 2006.

[5] Piot, E. and S. Tavoularis. Gap instability in laminar flows in eccentric annular channels. Nucl. Eng. Des., 241(11), 4615-4620, 2011.

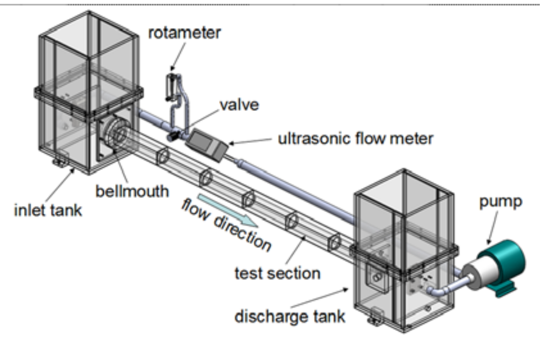

Figure 1. The experimental setup.

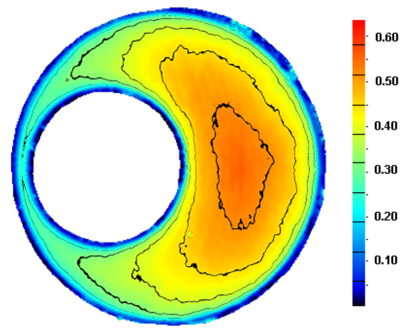

Figure 2. Time-averaged axial velocity contours.

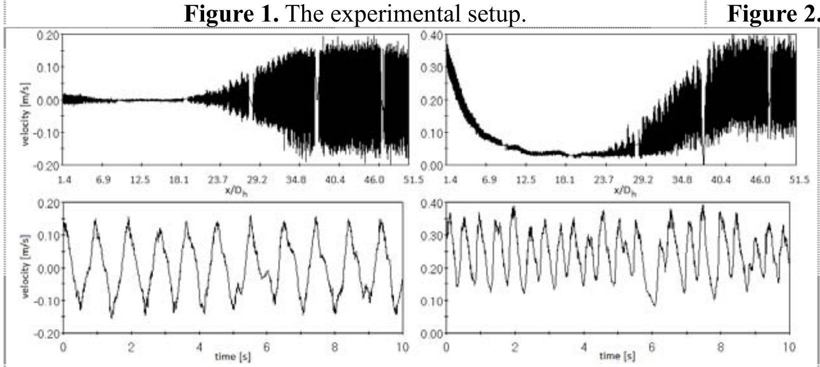

Figure 3. Cross- (left) and axial (right) flow velocity variations in the centre of the narrow gap along the test section (top) and at x/D_h = 51.4 (bottom); gaps in the signals appear at the joints between segments of the test section.

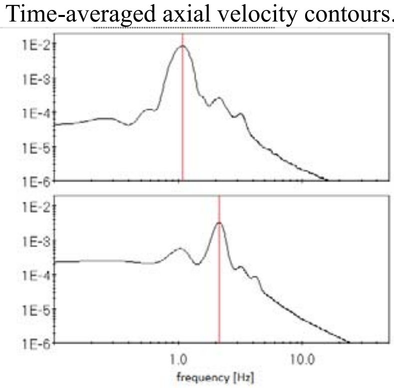

Figure 4. Power spectra of the cross- (top) and axial (bottom) flow velocity in the centre of narrow gap at x/D_h = 51.4.

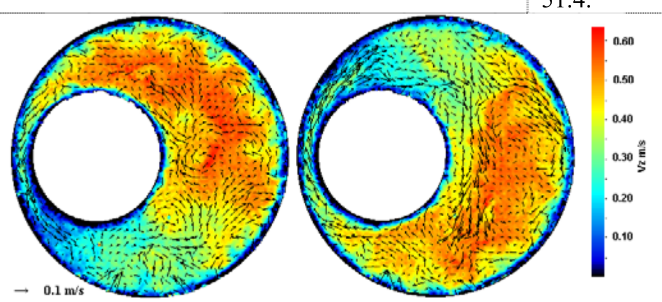

Figure 5. Two sets of instantaneous axial velocity contours and the corresponding transverse velocity vector maps at x/D_h = 54.2.